

Chemical Degradation of Indigo Potassium Tetrasulfonate Dye by Advanced Oxidation Processes

Veronica Camargo¹, Elba Ortiz^{1*}, Hugo Solis¹, Carlos M. Cortes-Romero²,
Sandra Loera-Serna¹, Carlos J. Perez¹

¹Department of Basic Sciences, Universidad Autónoma Metropolitana Azcapotzalco, Mexico City, Mexico

²Division of Industrial and Systems Engineering, Universidad Politecnica del Valle de México, Estado de México, Mexico

Email: *mariaelbaortiz@gmail.com

Received 3 August 2014; revised 1 September 2014; accepted 25 September 2014

Copyright © 2014 by authors and Scientific Research Publishing Inc.

This work is licensed under the Creative Commons Attribution International License (CC BY).

<http://creativecommons.org/licenses/by/4.0/>



Open Access

Abstract

The experimental degradation of a water soluble dye, potassium indigo tetrasulfonate salt, has been studied using stand-alone ozonation and photocatalytic oxidation process. Progress of the dye oxidation was followed by UV-VIS spectrophotometric measurements at controlled operating conditions. The organic content of reaction samples was measured to verify the process efficiency in dye mineralization. According to current results, almost complete color removal was obtained for ozonation within about 1 h reaction time. The reduction of the organic load was almost 80% from its original while initial sulphur content decreased to 32.5%. Dye conversion of 100% was obtained by means of a photocatalytic process using TiO₂ as catalyst at 294 nm irradiated UV light. This complete color removal for the catalytic process was observed within 7 min of reaction time. The calculated initial rate of reaction of photocatalysis treatment was 8 times faster than that of ozonolysis. However, the remaining organic load of photocatalysis was almost 88% from its original while the final sulphur content was 27.3%. This contrasting behavior of the performance of the type of oxidation process stressed importance of physicochemical phenomena and intermediates molecules present during dye degradation. An insightful and mechanistic aspect of the dye oxidation was developed by performing quantumchemical calculations.

Keywords

Indigo Potassium Tetrasulfonate, Advanced Oxidation Processes, Chemical Degradation, Theoretical Calculations

*Corresponding author.

1. Introduction

Nowadays, water pollution is the main concern of both research and governmental groups due to the increasing scarcity of drinking-water underground reserves and to the type and concentration of pollutant present in industrial wastewater. Textile industry represents one of the major environmental problems because it uses a large volume of the liquid and because the chemical compounds present in waste show resistance to elimination either by a biological or by chemical manner. For instance, dyeing of 1 kilogram of cloth needs at least 150 liter of water [1]. The presence of dye in water may have other environmental negative effects such as reflection of sunlight that impedes aquatic organisms to live and grow, affection to industrial plants economy due to the necessity of more numerous and effective water treatment plants, low quality of the treated water since the presence of residuals affect water properties such as pH, hardness, etc., non-soluble salts that cause partial or complete blocking of process tube lines which, in some cases, forces the plant to be stopped for hours or days for reparation [2]. In Mexico, for instances, governmental policies are becoming more strict concerning water treatment of textile industry wastes because water from these plants must be used for farming and cattle rising without further pollution problems. Nevertheless, some refractory aromatic compounds such as aniline and phenol are present in these effluents but in rather low concentration [3].

During extraction of the dye, irrespective of the technique(s) used, intermediaries, which, under ideal condition should be mineralized. Moreover, some of these organic intermediates could have a toxic effect on the bacteria used for wastewater purification, thereby affecting their ability to degrade [4] [5].

Recently, advanced oxidation processes (AOPs), in which oxygen-based radicals ($\bullet\text{OH}$, $\text{HO}_2\bullet$, and $\text{O}_2^-\bullet$) are generated *in situ* from water and O_2 , have been applied to dye degradation. These species take part in different reactions to degrade dye molecules completely. The processes are cleaner because dyes totally decompose to low-molecular-weight compounds (e.g., small aldehydes, carboxylic acids or small inorganic compounds), CO_2 , and H_2O , and no significant or solid secondary pollution is generated. Most applied techniques in AOPs are UV photolytic technique, Fenton process, photo-Fenton process, ozonation, sonolysis, photocatalysis, biodegradation and radiation-induced degradation of dyes as it is depicted in Figure 1 [6].

Other oxidizing reagents such as persulfate ($\text{S}_2\text{O}_8^{2-}$), chlorine (Cl_2), etc. may also be used in this way. AOPs are used either combined with each other or applied with different sorts of catalysts and photocatalysts homogeneously and heterogeneously. Therefore, a wide range of possible combinations could be introduced and evaluated for the oxidation of target pollutant molecules. The purpose of such combinations is the effective generation of hydroxyl radicals as non-selective oxidants which can highly oxidize almost all categories of chemical compounds. Mechanisms of the radical $\bullet\text{OH}$ formation in different AOP systems have been sufficiently described in many works [7] [8]. Due to the high energy costs involved in handling AOPs (ozone generation, light sources, pumps, etc.), they are still categorized as expensive processes in practice. Therefore, besides investigating the technical feasibility of these technologies in solving environmental problems [9], an economic feasibility study must be involved in each case of treatment. This important aspect, which can promote the commercialization of AOPs, is often neglected.

This paper deals with the mechanistic nature of the chemical degradation of commercial indigoid dye (potassium indigo tetrasulfonate salt) by performing both experimental work and theoretical calculations. Experimental dye oxidation is performed using oxidative techniques, namely, ozonation and photocatalysis, at controlled

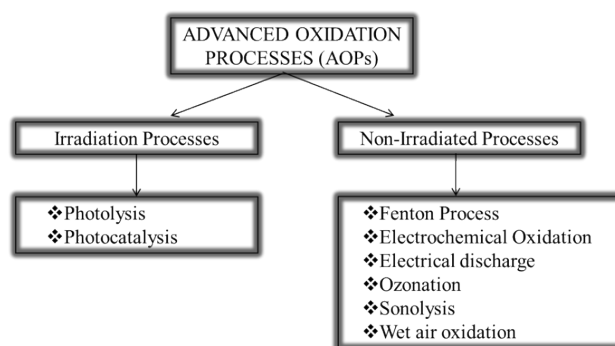


Figure 1. General scheme of advanced oxidation processes (AOPs).

and comparative reaction conditions. Comparison of effectiveness of the aforementioned techniques is reported based on a detailed analysis of results. In order to gain insight of the reaction mechanism and to support our current experimental results, theoretical calculations of the chemical stability for dye molecule were performed and results were discussed. Reaction products, regardless of the oxidative process, were analyzed with FTIR. Kinetics, as an empirical reaction law, was also performed using experimental data that led to a model equation.

2. Experimental Procedures

2.1. Reagents and Materials

The PITS (Aldrich Cat. 340596) was used with no further purification. Standard aqueous solution with 100 ppm of this compound was prepared and used in all experimental tests. Spectrophotometric analysis was performed using a Shimadzu Pharm Spec UV-VIS spectrometer. The UV-VIS spectrum is depicted in **Figure 2** as well as the calibration curve of the absorbance at 591 nm wavelength that is the maximal absorbance for the indigo dye aqueous solution. The linear behavior of the absorbance within the range of the operational dye concentration is also depicted in **Figure 2**. Quartz cells were used for these measurements to avoid interferences in absorbance lectures. The chemical oxygen demand (COD) analysis was that described in the HACH[®] manual using a standard kit of oxidant reagent within the range from 20 - 150 mg O₂/l. All the samples were treated similarly and the COD analyses were performed in a calibrated HACH[®] spectrometer model DRDL2400. Sulphur, as sulphates, was similarly determined with calibrated HACH[®] spectrometer. IR analysis of the reaction residuum was performed in a Cole-Parmer IR model.

2.2. Ozonation Procedure

Ozone was generated from pure oxygen using an Ozone O₃ Residual[®] Device for the current experimental work. The volumetric oxygen flow rate was kept constant and set in 0.40 liter per minute. This means that a total amount of ozone formed reaches 0.654 mol/h, which is more than that stoichiometrically required according to the amount of dye present in the reaction mixture. The simplified scheme and the actual experimental reactor are depicted in **Figure 3**. Glass reactor was provided of a gas inlet and purge to avoid pressure increases in the system since an accumulation of gas could occur. The gas-liquid reaction mixture was magnetically stirred to reduce the effect of reactant transport limitation, especially for ozone. Also, the continuous gas bubbling provokes turbulence in reaction mixture, which enhances proximity between the two phases. Room reaction temperature was used in experimentation. Sampling reaction was performed every 5 minutes to measure the amount of remaining dye by spectrophotometric analyses. The chemical oxygen demand (COD), pH and sulphur (as sulphates) were also measured for each sample.

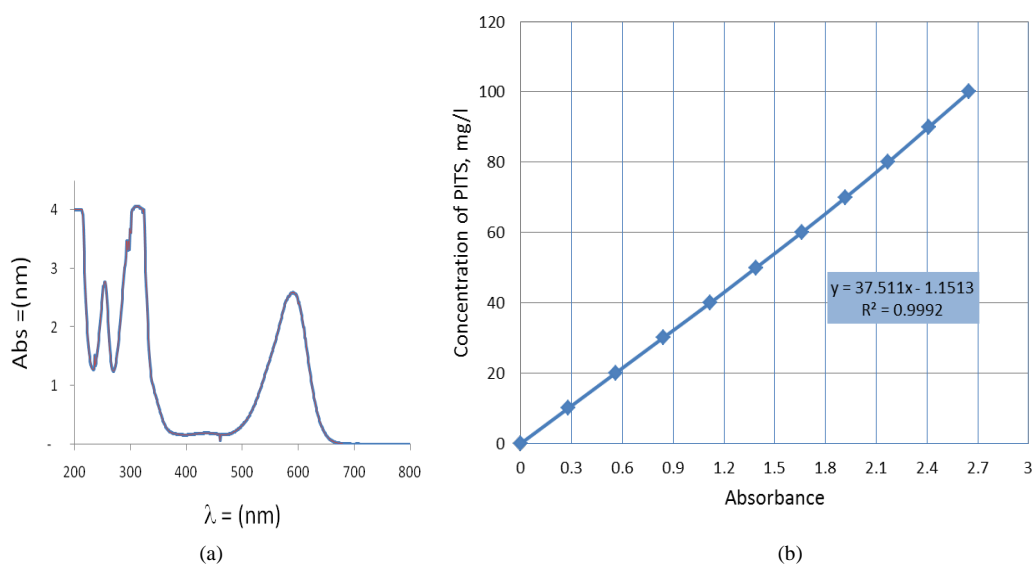


Figure 2. (a) UV-VIS spectrum of a 100 ppm aqueous solution of PITS; (b) Calibration curve of PITS at 591 nm.

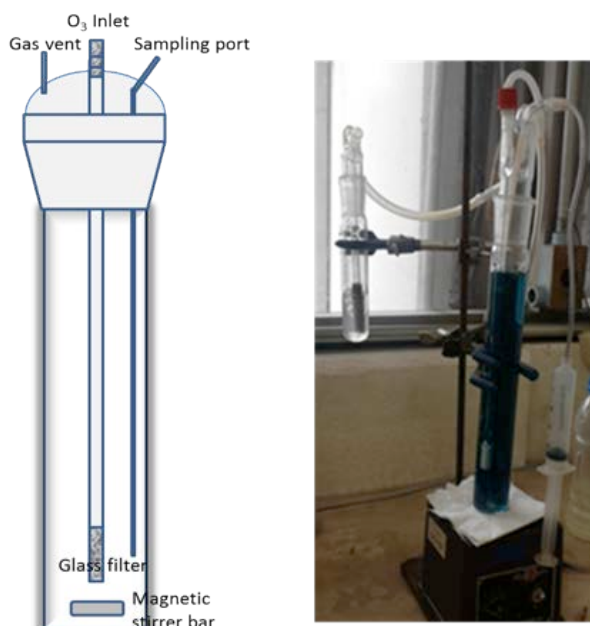


Figure 3. Experimental device for ozonolysis of PITS.

2.3. Photocatalysis Procedure

The catalytic reactor was a quartz cell that was treated in a dark chamber provided of a dual 254/365 nm UV lamp (Cole-Parmer, 8n watts, 115 V/60Hz and 0.16 A), see **Figure 4**. The amount of catalyst (TiO_2) was evaluated within the range of 10 - 30 mg (difference of 5 mg among experiments) using 10 ml of dye aqueous solution. The catalyst was pretreated similarly to a method reported elsewhere [10]. Basically, the catalyst was thermal treated to ensure that the rutile phase is obtained since it is the most stable polymorph of TiO_2 due to its lower total free energy than metastable phases of anatase or brookite. Reaction mixture was violently stirred under dark condition to reach the adsorption equilibrium during 10 minutes after that, UV-lamp was turn on and reaction. The amount of the catalyst was set in 30 mg from preliminary experimentation. It is necessary to stress that the experimental set-up was isolated with black paper to avoid influence of external light that could affect the reaction performance. Current experimental conditions were compared to those literatures reported by means of two runs at 254 nm and 365 nm for a qualitative evaluation of our reactor performance [11]. Advance of the photocatalytic reaction was followed by means of UV-VIS analysis; samples were taken at different times and the particles catalysts were removed by centrifugation. At current conditions reaction time was set at 7.5 minutes taking samples almost every minute or as soon as it was possible. The remaining dye concentration by UV-VIS spectrophotometry as well as the total organic load (COD).

2.4. Theoretical Calculations Procedure

The computational modelling of the different conformers were completely optimized by the local functional method (M05-2X), while for the transitions states and adducts, the calculations were carried out under unrestricted scheme (UM05-2X/6-31G (d, p)), developed by Truhlar group [12] [13], by using the 6-31G (d, p) basis set, implement in the Gaussian 09 package [14]. The complete set of electron for every atom was considered in our calculations, this is the so called all electron calculation. Has to be mention that all the theoretical results presented here were carried out taking into account the solvent effect by PCM solvent model. Calculation of frequencies for free molecules as well as for transition states was performed to verify these are minimal or maximum in potential energy surface (PES), respectively. From these results, the zero point energy corrections and standard Gibb's free energies (ΔG°) were considered. The molecular emission energy (UV spectrum) has been calculated as vertical transition energy of the ten lowest singlet vertical excitation energies and oscillator strengths by means the time-depending DFT (TDDFT) with the same functional and basis set as it is previously



Figure 4. Experimental dark chamber and quartz tubular reactor for photocatalysis of PITS.

described.

3. Results and Discussion

3.1. Experimental Results

Preliminary run tests were performed before presenting current results. By means of these experiments, it was observed that no significant degradation of the dyes is obtained with only the catalyst in the dark or with only UV irradiation without the catalyst. Hence, the degradation of the dye can be attributed to the catalytic effect, which results in the generation of charge carriers, viz., valence band holes and conduction band electrons, when TiO_2 is irradiated by UV light. The holes and electrons participate in the photocatalysis pathway resulting in the generation of hydroxyl ($\text{OH}\cdot$) radicals, which are the precursors of decomposition of any organic substrate.

Figure 5 shows the comparative dye oxidation progress by means of the photocolometric curve at 591 nm for both ozonation and photocatalytic processes. It can be observed that the complete color removal is obtained for the catalytic process while a maximum 93.1% color removal is obtained for the ozonation one. The steep line of the catalytic treatment indicates that reaction rate is much higher than that of ozonation of which the line is rather smooth. Regression of these curves led to an empiric kinetic law from which initial reaction rate can be calculated. Doing so, the rate of the catalytic reaction was $18.3 \text{ mg}\cdot\text{l}^{-1}\cdot\text{min}^{-1}$ while for ozonolysis was $2.13 \text{ mg}\cdot\text{l}^{-1}\cdot\text{min}^{-1}$. Hence, the rate of the reaction by photocatalysis is almost eight times faster than that by ozonolysis. It is well known that ozonolysis is a transport limited process since ozone must shift from gas to liquid phase for the reaction to take place. Not only the operating conditions, such as temperature and pressure, are important for this gas mass transport, but also the level of turbulence present in the reaction mixture. Care must be taken of ensuring that ozone is available at the liquid phase and that is the role of stirring and bubbling to provide enough molecular movement between heterogeneous phases. The linearity of the reaction progress indicates that, even if the reaction is transport limited, this effect is constant during our complete experiment.

Concerning the residual organic molecules, **Table 1** shows the result of the chemical oxygen demand and sulphur content of the product of both ozonation and photocatalysis processes. Mechanistically, hydroxyl species oxidize the dye through the formation of colorless intermediates, which on prolonged exposure to the active oxidant agent should lead to CO_2 , H_2O , N_2 and other inorganic ions such as ammonium (NH_4^+), nitrate (NO_3^-) and sulphate (SO_4^{2-}) species. Although a complete color removal is observed for the catalytic process in a rather short time, only a partial degradation of the dye molecule is obtained as it can be inferred from the result of the remaining organic load. On the other hand, the residual organic load for the ozonolysis is lower than that of photocatalysis which indicates that the dye molecule undergoes further degradation due to the presence of ozone

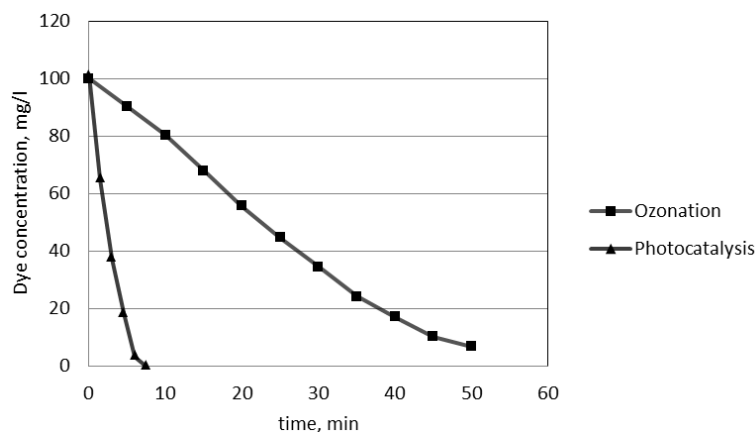


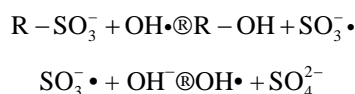
Figure 5. Dye oxidation progress for both photocatalysis and ozonation processes at similar reaction conditions. TiO_2 as catalyst and UV light (295 nm wavelength) were used in photocatalysis while ozone was produced *in situ*.

Table 1. Residual organic load and sulphur content of the experimental degradation of PITS using two AOP's.

AOP	Reaction time [min]	Remaining % organic load, as COD	Remaining % S, as sulphates
Photocatalysis	7.5	87.8	27.3
Ozonolysis	50	20.1	32.5

and, more important, due to the longer reaction time.

It is well known that the initial step in the sulphonated dye degradation involves the formation of harmless sulfate ions (SO_4^{2-}). These are formed by the cleavage of C-S bond to form SO_3^\bullet , followed by the reaction with hydroxyl anions (OH^-). The reactions can be represented as follows [15]:



where R corresponds to any alkyl or aryl group. Hence, the relative ease with which these sulfate ions are formed in the initial step is detrimental to the further breakdown of the dye structure due to other reactions like hydroxylation, oxidation and decarboxylation. In this regard, the point of attachment of the sulfo group in the dye plays a major role. Therefore, since the S content is similar for both oxidation techniques, it can be concluded that reactivity of sulphonic group is relatively higher than the rest of the functional groups, except for the double bond scission that occurs in a rather higher reaction rate.

3.2. Theoretical Calculations Results

The optimized geometry of the structural isomers of tetrasulphonated indigo molecule was calculated and depicted in **Figure 6**. Two possible structural isomers were considered, the first where the pyrrole groups are located at different side of a horizontal plane in the molecule, named *trans*NN (a); and the other with these functional groups at the same side of the horizontal plane in molecule, named *cis*NN (b). There is a third possible structural isomer and that is the one with central double bond shifted to one side of the molecule. This means that nitrogen forms an imino group that is located to one side of the molecule, see **Figure 6(c)** and **Figure 6(d)**. Actually, the latter molecule is a resonance structure around the central double bond. The result of this electron movement is a rupture in the molecular symmetry, which makes it to gain certain degree of mobility (rotation) around the central bond.

According to the Gibbs free energy of the three possible structures, the most stable structure was *trans*NN, *i.e.*, with pyrrole groups on the opposite side of the horizontal molecular plane. *Trans*NN corresponds to the reference in energy value. This means that the energy value of *cis*NN is $27.4 \text{ kJ}\cdot\text{mol}^{-1}$ higher than that from reference, which is the value, indicated in **Figure 6**. Concerning the resonance structure (c) and (d), the energy value

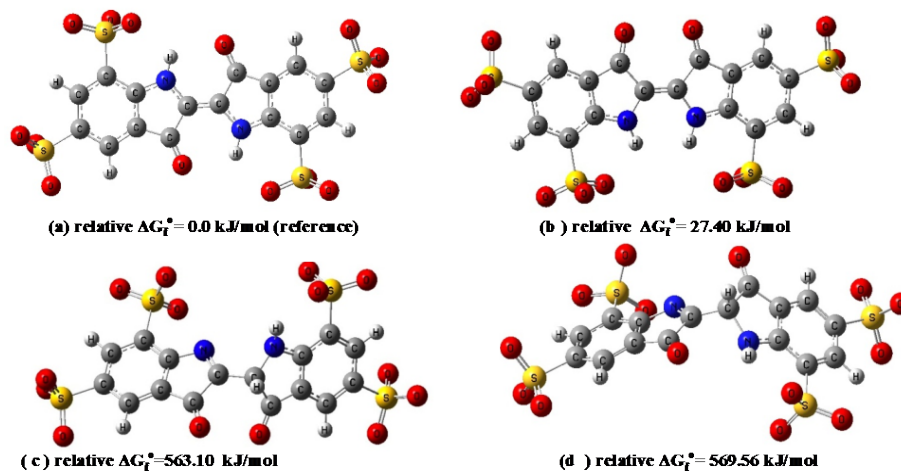


Figure 6. Structural isomers used for quantumchemical calculations. (a) *Trans*NN; (b) *Cis*NN; (c) *Cis* molecule with imino group; and (d) *Trans* molecule with imino group.

reaches 563 and 569 $\text{kJ}\cdot\text{mol}^{-1}$, respectively. This is an indication that formation and stability of an imino group requires high energy, which obviously depends on operating conditions. Nevertheless, the lower energy value of the *trans*NN is owing to resonance through the whole molecule that is also observed from the orbital total conjugation, **Figure 7**. The electronic movement within the molecule is best described with HOMO-LUMO distribution. According to the HOMO electronic distribution for both *trans* and *cis* molecule, resonance of double bond describes a dorsal spine through the whole molecule regardless the location of the nitrogen atom. Also, it can be inferred from the HOMO distribution that interaction between the carbonyl group and the amino group stabilizes the molecule in the case of the *trans*NN while for *cis*NN this interaction does not occur.

The electrostatic potential (EP) for most stable *trans*NN depicted in **Figure 8** confirms the uniformity of the electronic distribution that provokes stability within the molecule. This result indicates that the molecule is susceptible to react through any of its functional groups with no preference to one, even to the double bond, that could be expected to be the most reactive one. It is important to mention that, even in undergraduate textbooks, Ozonation is the route of reaction of aliphatic double bond, which produces two carbonyl groups by dividing the molecule [16].

Together with the electronic distribution through the whole molecule, the UV-VIS spectrum was also calculated and explained according to the obtained bands. From **Figure 8**, the green color relates the π conjugation system. The excitations that are responsible of blue color of indigo present a $\pi-\pi^*$ character with a large oscillator strength. Then the ten lowest singlet vertical excitation energies and oscillator strengths from the TD-DFT calculations were used to predict the UV-VIS spectrum for the indigo tetrasulphonate molecule through the fitting of a Gaussian (with the GaussView default parameters for half-width) centered at the computed excitation energies. The predicted UV-VIS spectrum with the PCM solvent model was plotted and the λ_{max} values in each case are summarized in **Table 2**.

The reported λ_{max} corresponds to the transition energy from the ground electronic state to the first dipole-allowed excited state in this case HOMO \rightarrow LUMO excitation, see **Table 2**. In addition, the other contribution obtained from the calculated spectra, but those signals are outside of the visible electromagnetic field. According to the calculated spectrum (**Figure 9**) for the *trans*NN isomer, it can be observed that the blue shift occurs at 508 nm which is shifted from that experimentally obtained (591 nm).

4. Conclusion

The color removal of a model textile wastewater in which indigo tetrasulphonated dye is dissolved occurs faster by means of a catalytic oxidation process than using ozone as oxidant agent. However, the remaining carbon load is considerable which indicates that only the chromophore group has reacted but still organic intermediate molecules have not reacted. The sulphonic group appears as the most prompt functional group for oxidation since the remaining sulphur is similar for both processes, even though the catalytic process has been stopped in less than 10 minutes of reaction time while ozonolysis reached 50 minutes. The theoretical calculation indicated

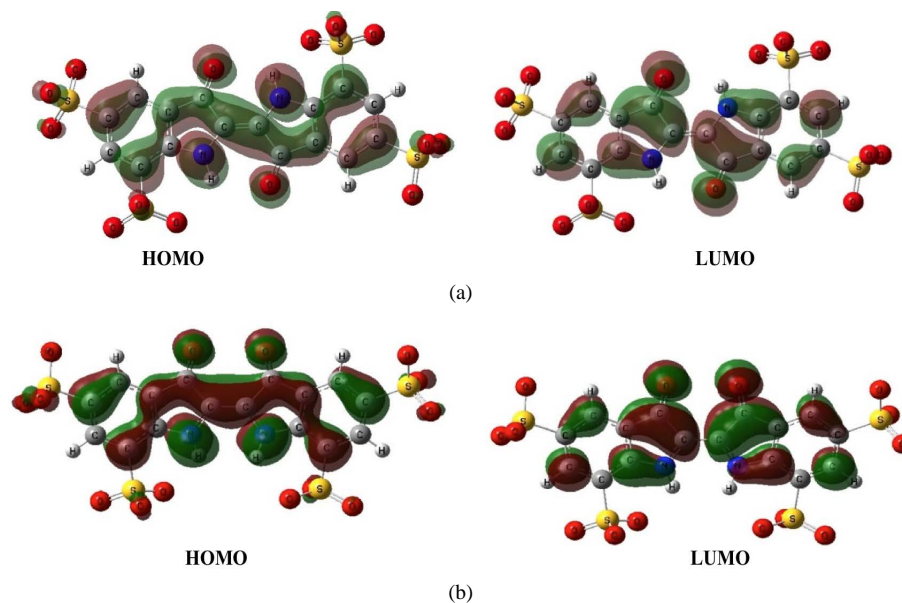


Figure 7. Molecular orbital distribution of structural isomers of indigo tetrasulphonate dye. Value of isosurface 0.02. (a) *Trans*NN; (b) *Cis*NN.

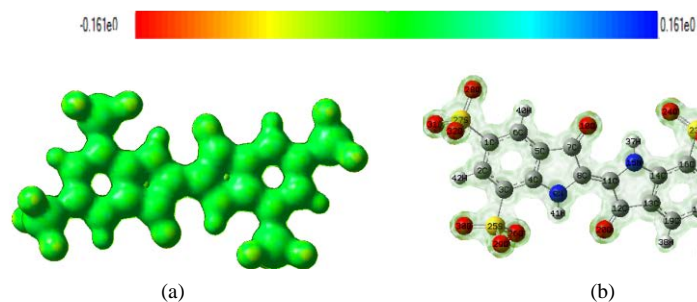


Figure 8. Electrostatic potential (EP) scheme for *trans*NN. The color scale corresponds to the isosurface obtained in the molecule. (a) Color distribution; (b) Atoms and functional groups.

Table 2. Calculated UV-VIS bands of indigo tetrasulphonated molecule.

Species	Method TD-DFT/PCM λ_{\max} [nm]	Oscillator Strength	Energies and Oscillator Strengths	Experimental Reported [1] λ_{\max} [nm]
Indigo	508.51	0.4369	148 149 Singlet (HOMO→LUMO)	591
	282.51	1.0137	147 149 Singlet (HOMO-1→LUMO)	320
			146 149 Singlet (HOMO-2→LUMO)	
145 149 Singlet (HOMO-3→LUMO)				
144 149 Singlet (HOMO-4→LUMO)				
251.32	0.5974	144 149 Singlet (HOMO→LUMO) 148 151 Singlet (HOMO→LUMO + 2)	250	

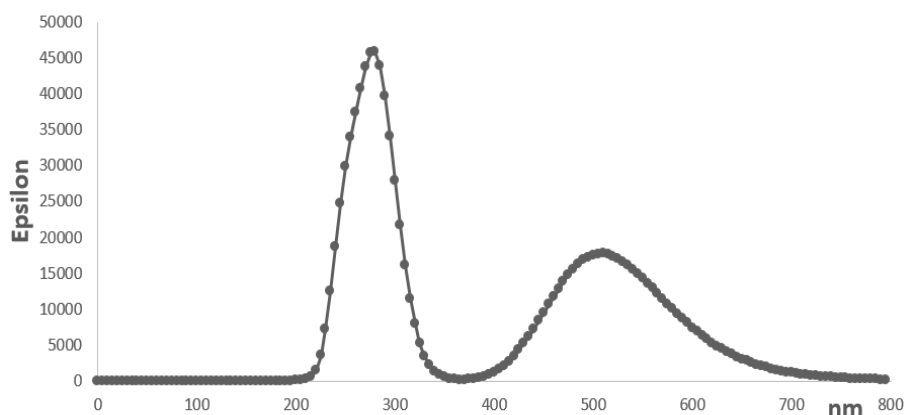


Figure 9. Calculated UV-VIS spectrum of indigo tetrasulphonate molecule.

that regardless of the structural configuration of the dye molecule, it reacts through the same pathway since the complete set of functional groups is susceptible to be oxidized.

References

- [1] Mansilla, H.D., Lizama, C., Gutarra, A. and Rodríguez, J. (2001) Treatment of Liquid Waste from the Pulp and Textiles. Blesa, M., Ed., CYTED VIII-G, Buenos Aires, Chapter 13. <http://www.aguasinfronteras.org/PDF/DESINFECCION%20Y%20DESCONTAMINACION.pdf>
- [2] Yonar, T. (2011) Decolorisation of Textile Dyeing Effluents Using Advanced Oxidation Processes. Hauser, P.J., Ed., Environmental Engineering Department, Uludag University, Bursa. <http://cdn.intechopen.com/pdfs-wm/22391.pdf>
- [3] INEGI: National Institute of Statistics and Geography (2010-2011) The Textile and Clothing Industry in Mexico. Serie Sector Statistics.
- [4] Bazin, I., Hassine, A.I.H., Hamouda, Y.H., Mnif, W., Bartegi, A., Ferber, M.L., Waard, M. and Gonzalez, C. (2012) Estrogenic and Anti-Estrogenic Activity of 23 Commercial Textile Dyes. *Ecotoxicology and Environmental Safety*, **85**, 131-136. <http://dx.doi.org/10.1016/j.ecoenv.2012.08.003>
- [5] Zhao, Y.H., Zhang, X.J., Wen, Y., Sun, F.T., Guo, Z., Qin, W.C., Qin, H.W., Xu, J.L., Sheng, L.X. and Abraham, M.H. (2010) Toxicity of Organic Chemicals to *Tetrahymena pyriformis*: Effect of Polarity and Ionization on Toxicity. *Chemosphere*, **79**, 72-77. <http://dx.doi.org/10.1016/j.chemosphere.2009.12.055>
- [6] Hisaindee, S., Meetani, M.A. and Rauf, M.A. (2013) Application of LC-MS to the Analysis of Advanced Oxidation Process (AOP) Degradation of Dye Products and Reaction Mechanisms. *TrAC Trends in Analytical Chemistry*, **49**, 31-44. <http://dx.doi.org/10.1016/j.trac.2013.03.011>
- [7] Chong, M.N., Jin, B., Chow, C.W.K. and Saint, C. (2010) Recent Developments in Photocatalytic Water Treatment Technology: A Review. *Water Research*, **44**, 2997-3027. <http://dx.doi.org/10.1016/j.watres.2010.02.039>
- [8] Agustina, T.E., Ang, H.M. and Vareek, V.K. (2005) A Review of Synergistic Effect of Photocatalysis and Ozonation on Wastewater Treatment: A Review. *Journal of Photochemistry and Photobiology C: Photochemistry Reviews*, **6**, 264-273. <http://dx.doi.org/10.1016/j.jphotochemrev.2005.12.003>
- [9] Chong, M.N., Sharma, A.K., Burn, S. and Saint, C.P. (2012) Feasibility Study on the Application of Advanced Oxidation Technologies for Decentralised Wastewater Treatment. *Journal of Cleaner Production*, **35**, 230-238. <http://dx.doi.org/10.1016/j.jclepro.2012.06.003>
- [10] Gómez-Solis, C., Juárez-Ramírez, I., Moctezuma, E. and Torres-Martínez, L.M. (2012) Photodegradation of Indigo Carmine and Methylene Blue Dyes in Aqueous Solution by SiC-TiO₂ Catalysts Prepared by Sol-Gel. *Journal of Hazardous Materials*, **217-218**, 194-199. <http://dx.doi.org/10.1016/j.jhazmat.2012.03.019>
- [11] Sajan, C.P., Basavalingu, B., Ananda, S. and Byrappa, K. (2011) Comparative Study on the Photodegradation of Indigo Carmine Dye Using Commercial TiO₂ and Natural Rutile. *Journal of the Geological Society of India*, **77**, 82-88. <http://dx.doi.org/10.1007/s12594-011-0010-y>
- [12] Zhao, Y. and Truhlar, D.G. (2008) The M06 Suite of Density Functionals for Main Group Thermochemistry, Kinetics, Noncovalent Interactions, Excited States, and Transition Elements: Two New Functionals and Systematic Testing of Four M06 Functionals and Twelve Other Functionals. *Theoretical Chemistry Accounts*, **120**, 215-241. <http://dx.doi.org/10.1007/s00214-007-0310-x>

- [13] Zhao, Y., Schultz, N.E. and Truhlar, D.G. (2005) Exchange-Correlation Functional with Broad Accuracy for Metallic and Nonmetallic Compounds, Kinetics, and Noncovalent Interactions. *The Journal of Chemical Physics*, **123**, Article ID: 161103. <http://dx.doi.org/10.1063/1.2126975>
- [14] Frisch, M.J., Trucks, G.W., Schlegel, H.B., Scuseria, G.E., Robb, M.A., Cheeseman, J.R., Scalmani, G., Barone, V., Mennucci, B., Petersson, G.A., Nakatsuji, H., Caricato, M., Li, X., Hratchian, H.P., Izmaylov, A.F., Bloino, J., Zheng, G., Sonnenberg, J.L., Hada, M., Ehara, M., Toyota, K., Fukuda, R., Hasegawa, J., Ishida, M., Nakajima, T., Honda, Y., Kitao, O., Nakai, H., Vreven, T., Montgomery Jr., J.A., Peralta, J.E., Ogliaro, F., Bearpark, M., Heyd, J.J., Brothers, E., Kudin, K.N., Staroverov, V.N., Kobayashi, R., Normand, J., Raghavachari, K., Rendell, A., Burant, J.C., Iyengar, S.S., Tomasi, J., Cossi, M., Rega, N., Millam, N.J., Klene, M., Knox, J.E., Cross, J.B., Bakken, V., Adamo, C., Jaramillo, J., Gomperts, R., Stratmann, R.E., Yazyev, O., Austin, A.J., Cammi, R., Pomelli, C., Ochterski, J.W., Martin, R.L., Morokuma, K., Zakrzewski, V.G., Voth, G.A., Salvador, P., Dannenberg, J.J., Dapprich, S., Daniels, A.D., Farkas, O., Foresman, J.B., Ortiz, J.V., Cioslowski, J. and Fox, D.J. (2009) Gaussian 09, Revision A.1. Gaussian, Wallingford.
- [15] Rauf, M.A. and Ashraf, S.S. (2009) Fundamental Principles and Application of Heterogeneous Photocatalytic Degradation of Dyes in Solution. *Chemical Engineering Journal*, **151**, 10-18. <http://dx.org/10.1016/j.cej.2009.02.026>
- [16] McMurry, J. (2008) Organic Chemistry. 7th Edition, Thomson Brooks Cole.

Scientific Research Publishing (SCIRP) is one of the largest Open Access journal publishers. It is currently publishing more than 200 open access, online, peer-reviewed journals covering a wide range of academic disciplines. SCIRP serves the worldwide academic communities and contributes to the progress and application of science with its publication.

Other selected journals from SCIRP are listed as below. Submit your manuscript to us via either submit@scirp.org or [Online Submission Portal](#).

